Proceedings of the ASME 2021 16th International Manufacturing Science and Engineering Conference
MSEC2021
June 21-25, 2021, Virtual, Online

MSEC2021-63823

A COMPUTATIONAL STUDY ON NOVEL RUNNER EXTENSION DESIGNS VIA 3D SAND-PRINTING TO IMPROVE CASTING PERFORMANCE

Ryan Stebbins, Philip King, Guha Manogharan*
Department of Mechanical Engineering
Pennsylvania State University, University Park, PA 16801
*Corresponding author: gum53@psu.edu

ABSTRACT

3D sand-printing (3DSP) has become more popular in foundry applications due to its ability to create complex gating geometries. Since filling related defects, like entrained air and bi-films, are most commonly caused by high melt velocity and turbulence, recent 3DSP research has focused on designing gating systems to reduce melt velocity and turbulence. However, there have been no reported efforts on advancements in the design of runner extensions as a method to improve casting quality, despite its tremendous impact on the initial metal flow characteristics. The ability to fabricate 3DSP molds allow for unique runner extension designs that aid in improving casting quality. This paper is the first study known to the authors that investigates novel 3D runner extension designs to determine the most effective design for reducing sand casting defects. Based on literature review and design principles developed for 3D sprue geometries, six different runner extensions were studied using Computational Fluid Dynamics (CFD) modeling for foundry pouring conditions. The designs were evaluated on their ability to reduce defects like entrained air and bubbles, as well as to prevent backflow and reflected waves. An unweighted ranking matrix and comparison matrix against the control (straight runner extension) has been established based on air entrainment, tracer, voids, and extension volume. The results showed that the by-pass principal and surge control systems are effective at reducing reflective waves and controlling the ingate flow. The novel 3D duckbill trap extension proposed in this study had the best overall performance based on a 16% reduction in entrained air and a 71% reduction in void particles in the casting volume compared to the control extension design. These results provide a framework to further optimize runner extensions, utilize the advantages of 3D Sand-Printing technology to improve mechanical strength and reduce filling defects in sand-casting.

1. INTRODUCTION

Sand casting has been used for thousands of years and is one of the most common manufacturing methods[1],[2]. Its ability to quickly and economically produce near-net shape geometries made out of a broad range of alloys distinguishes it from other manufacturing methods. Almost 90% of manufactured products contain one or more casting resulting in the metal casting industry having a $110 billion economic impact in the United States and employing 160,000 Americans in 2019[2],[3].

In the last decade, additive manufacturing (AM) has become a growing area of manufacturing due to its ability to create complex geometries with little material waste. Research in AM has grown rapidly and continued advancements are expected [4]. AM binder jetting technology, i.e. 3D sand-printing (3DSP), has emerged as an alternative method for mold production because of its ability to create complex shapes and internal cavities[5], [6]. This allows for new gating and riser designs that are not possible via traditional patterns[7],[8].

In the past, researchers have proposed sand mold design guidelines to assist foundries on traditional 2D gating and riser design[9]. Gating systems, which include sprues, runners, ingates, and runner extensions, seen in Figure 1, are designed to facilitate quiescent filling of the casting cavity. It is imperative that gating systems reduce flow velocity and fill the mold quiescently, while minimizing surface turbulence, since velocity and turbulence are the most common causes of filling related defects[10]. Past research on gating design has primarily focused on sprues, runners and ingates, with little emphasis on runner extensions[11],[12],[13].

Runner extensions, as the name implies, are extensions of the runner system past the ingates. Their primary function is to utilize the initial melt's momentum to trap and prevent casting defects from entering the main casting[9]. The initial melt is typically the coldest and "dirtiest" metal, containing the most air and oxide entrapments due to high velocities and turbulent pouring[9]. The secondary function of a runner extension is to reduce reflecting waves resulting from the impact of the initial melt against the end of the runner[14]. Traps (also known as end dumps, slag or dross traps, flow off dump, and surge control systems) are similar to runner extensions because they are typically attached to the end of runners to trap the initial melt, entrained air, oxides, sand or other debris[9]. Figure 2 illustrates the difference between the runner extension and trap. Once runner extensions are filled, they no longer aid in reducing turbulence, velocity, or in trapping entrainments. This also

applies for traps because they can no longer trap defects and debris after being filled.

An ideally designed runner extension should reduce the incoming metal's velocity and turbulence, prevent the formation of defects and initial impurities from entering the casting. However, due to a lack of research, there is no consensus on the proper design of a runner extension.

The motivation for this paper is to systematically study novel runner extensions that could be achieved by traditional and/or 3DSP mold making processes to reduce sand casting defects. Using Flow-3D Cast (Flow Science Inc, v5.0, Santa Fe, NM) computational fluid dynamics (CFD) software, multiple new design concepts for runner extensions were simulated and evaluated to determine the best design candidate for defect reduction.

In Section 2, a brief literature review is presented on casting defects, best practices in casting and mold design, and current state of reported research in runner design methodology. Section 3 details the methodology employed in this computational study on runner extension design concepts in Flow-3D Cast. Section 4 presents the results and data from the simulations. Section 5 discusses the implications of the findings in terms of reducing casting defects and improving casting quality. Section 6 summarizes major research findings, implications, limitations and future direction for this research.

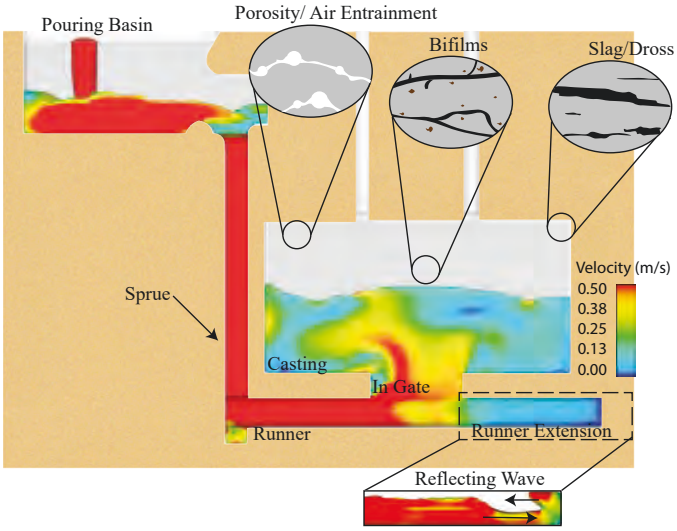

Figure 1: Schematic of gravity feed traditional sand casting with control runner extension geometry

2. LITERATURE REVIEW

There are many factors that influence a casting's tendency to develop defects during filling. This paper will focus on defects caused by high ingate velocity and surface turbulence. It has been shown that if the maximum critical velocity at the ingate (0.5 m/s for most metals) is exceeded, destabilizing forces are generated to overcome surface tension and gravity which results in surface turbulence and oxide formation [15],[9],[10]. Foundries with turbulent filling experience 20-25% scrap rates, with about 15% of those associated with random inclusions and porosity[9].

Higher velocity and turbulence have an impact on the formation of defects, particularly double sided entrained oxide films or bi-films, as referred to by Campbell[10]. Reactive metals like aluminum naturally form a protective oxide skin on their surface. However, during turbulent filling waves can cause the metal to fold and splash which traps the surface oxide films in the melt and forms bi-films. These bi-films eventually create cracks in the casting leading to reduced mechanical strength and ductility. [15],[16].

Such turbulent and folding waves that cause bi-films, also trap air and bubbles in the melt. Consequently, entrained air and bubbles are always accompanied by the presence of bi-films[10]. Air bubbles are trapped in the melt due to the reduction of buoyancy from oxygen consumption during oxidation reaction with the metal [10]. If the air bubbles escape the melt and float to the surface, they can leave behind a trail of elongated bi-films[10]. About 80% of all defects are caused by porosity and gas entrapment, which are almost always caused by air entrainment and trapped bubbles due to turbulence[10]. In a study on the fatigue limit of die cast magnesium and aluminum alloys, researchers found that 98.5% of the specimen's fatigue cracks were initiated at locations of porosity[17]. Another study found that fatigue resistance of cast aluminum relies heavily on the presence of defects. The most influential defect was determined to be porosity located near the surface of the specimens, which accelerates the fatigue damage[18].

Reflecting (also called returning) waves are another major issue during filling. After impacting the end of the runner or runner extension, the momentum of the initial melt causes a backflowing wave as shown in the inset of Figure 1. In reflecting waves, hydraulic jumps are generated which causes the formation of entrapped air and bi-films[14]. These reflecting waves also carry trapped defects back from the extension and into the casting, making the runner extension ultimately ineffective and even more detrimental than the runner[9].

There have been very few studies on systematically studying the design and effectiveness of runner extensions, for the purpose of reducing entrainment, turbulence and velocity. To the best of their knowledge, the authors are not aware of reported studies that have leveraged 3DSP to develop and evaluate novel runner extension designs.

Past research has only evaluated the effectiveness of traditional traps. According to Campbell, traditional traps are ineffective because of their inability to trap defects and prevent reflecting waves[9]. However, he has described several variations of runner extensions, traps, and surge control systems to combat these issues in two casting handbooks[9],[11],[13]. Most notable were his vortex system for runners and gates, and his surge control systems. The vortex system benefits from the organized flow of vortexes. This has been shown (via computational simulation) to be effective during higher velocity flow, typically seen in the early stages of filling. Surge control systems take advantage of the by-pass principal, which describes the diversion of the initial melt away from the ingate to control

the initial flow velocity[9],[13]. Additionally, the by-pass principal can be used to gradually build pressure in the runner, reducing the likelihood of a reflecting wave. Campbell describes a novel surge control system, labeled vortex surge cylinder, that utilizes vortices and the by-pass principal to control the melt's flow and speed[9]. In another study by Ashton and Burr on runner extensions, it has been shown that runner extensions performed poorly at trapping dirt due to reflecting waves[9].

Dai et al. have investigated the cross sectional geometry of traditional runner systems to evaluate their effects on the mechanical properties of Al-7Si-Mg. Three different runner systems were analyzed using Flow 3D CFD simulations. The experimental plan included X-ray radiography and four-point bending tests. It was determined that the vortex runner system performed better than a rectangular and triangular shaped runner, reducing turbulence, and entrapment defects, while improving Al-7Si-Mg mechanical strength. Dai et al. credited the superior performance of the vortex system to the organized flow of the melt[19].

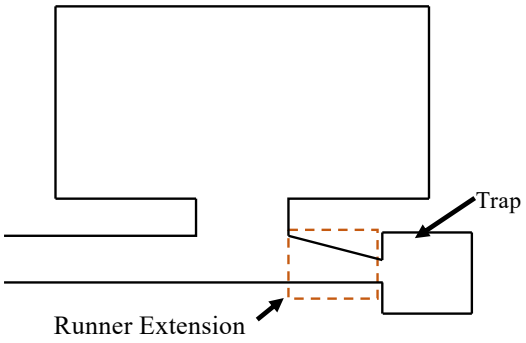

Figure 2: Difference between runner extension and a trap

In another study, the manufacturer Komatsu employed CFD simulations to reduce the number of inclusions in the casting through different extension and trap designs. They reduced the amount of inclusions by 60-95%, using a choked runner extension and an end trap. It was found that choked extensions performed better than non-choked runners, and the addition of a trap at the end of the extension further improved the performance due to the added volume for trapping inclusions[20].

Recent research has been done evaluating Campbell's runner and gating system designs, using computational simulation for evaluation and comparison[21]. Average entrained air volume, average surface defect concentration, velocity, and casting weight were analyzed. It was found that Campbell's trident and vortex gates performed better than the vertical gate, but at the cost of reduced yield.

Recent work has investigated novel sprue geometries by leveraging 3DSP to print sand molds. Designs were compared using CFD modeling, CT scans, microstructure and inclusion characterization, and three-point bending tests. Based on the results, their conical helix sprue reduced the casting defect volume by 99.5% and exhibited a 35% reduction in inclusions compared to a traditional straight sprue. Additionally, they saw a 8.4% increase in average ultimate flexural strength compared to the traditionally designed sprue casting[8].

3. METHODOLOGY

3.1 Runner Extension System Design

The vortex runner system, as previously discussed, was used as the control design to compare the effectiveness of the simulated runner extensions in this study[19]. Five other novel extension and trap systems were created and evaluated: fan trap (Figure 3(b)), vortex surge cylinder (or vortex cylinder) (Figure 3(c)), duckbill trap (Figure 3(d)), conical helix (Figure 3(e)), and split conical helix (Figure 3(f)). The fan trap was inspired by Campbell's bottom connected vertical fan gate [9]. The vortex surge cylinder is another one of Campbell's concepts[9]. Komatsu's findings of the effectiveness of a choked extension and rectangular trap inspired the duckbill trap[20]. Both the conical helix and split conical helix extensions are original 3D designs derived from the research previously mentioned on novel sprues, specifically the conical helix sprue[8]. The volumes of each extension design, shown in Table 1, were recorded to compare casting yield.

The inlet diameter of each extension design was uniform to ensure similar runner diameter. Each runner extension is part of the same mold design (pouring basin, sprue, runner and mold cavity) to isolate the effects of the studied runner extensions on entrained air mass, number of void particles, amount of tracer particles, backflow, and velocity. The casting and runner dimensions were benchmarked against Campbell's vortex runner system setup[19], shown in Figure 3(a). The sprue design and dimensions were adopted from Sama et al.'s paper on novel sprue designs[8].

It is intended that runner extensions with higher design complexity, seen in Figure 3 (c), (e), and (f), will be produced via 3DSP using silica sand and furan resin. The more symmetric and simple geometries, seen in Figure 3 (a), (b), and (d) will be created using traditional green sand methods. It is not expected that this will affect outcomes during future experimentation, since runner extensions are scrapped post casting and are used only for initial flow control.

Table 1. Runner extension volumes and the percent difference in volume against the control

Extension	Extension Volume	% Volume Difference
Control	28,274 mm³	0%
Fan Trap	33,236 mm³	17.5%
Vortex Cylinder	57,322 mm³	102.7%
Duckbill Trap	51,935 mm³	83.7%
Conical Helix	26,542 mm³	-2.6%
Split Conical Helix	45,660 mm³	61.5%

3.2 Simulation

Filling simulations were conducted using Flow 3-D Cast v5.0 CFD software. The metal and mold material chosen were Al 319 and furan bonded silica sand, respectively, using material

properties in Flow-3D Cast's database. A constant filling rate, that is reflective of on-going experimental runs, of 0.000225 m³/s was used at a pouring temperature of 685°C. A hexahedral mesh grid with a cell size of 1.5mm was used for simulation. This ensured a minimum of three cells across the thinnest sections of the casting as shown in Figure 3. Simulation parameters are summarized in Table 2. A sampling volume was created, as shown in Figure 4, to define the casting cavity and compute the total entrained air, void particles, and tracer particles present. Sampling volumes are 3D data collection regions and does not have any effect on the fluid field. They are used to count particles, measure forces, and other parameters. Only data within the volume covered by the sampling volume component is analyzed in this study[22].

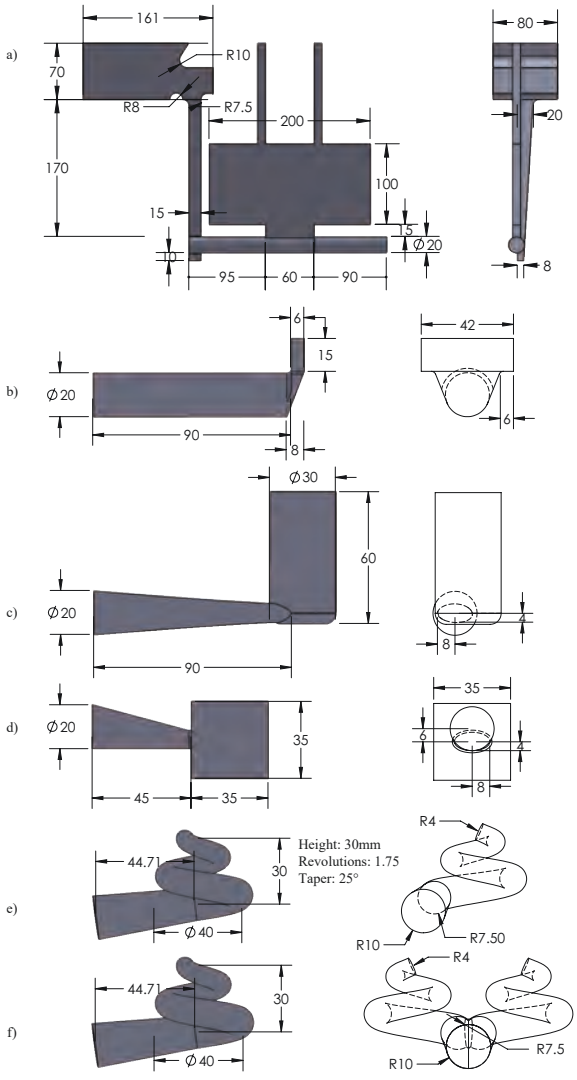

Figure 3: Simulation casting dimension in mm with control extension dimensions (a), fan trap extension dimensions (b), vortex cylinder extension dimensions (c), duckbill extension dimensions (d), conical helix dimensions (e), split conical helix dimensions (f).

The primary focus of the entrainment model is to compute the air entrainment caused by the turbulence at a free surface. The rate at which air is entrained is estimated by balancing the stabilizing fluid forces, gravity and surface tension, and destabilizing force, turbulence[22]. Air entrainment can physically represent porosity and surface finish defects that develop during filling. A 100% porous baffle is used as a flux surface to count and track the backflow of metal from the extension into the casting cavity, without affecting the melt flow[22]. Any fluid that passes through the flux surface is marked and traced as it flows throughout the casting to evaluate the effectiveness of the runner extension in capturing and retaining the initial melt. Voids are regions without fluid mass, physically representing regions filled with a vapor or gas with densities dissimilar from melt (fluid) density. Once these regions are no longer resolvable by the mesh, 3 to 4 mesh cells across are considered to be collapsed and can be tracked as void particles[22]. This represents the movements of finer pockets of air or bubbles within the casting.

Table 2. Simulation parameters

Mesh Size	1.5 mm
Pouring Temperature	685ºC
Air Temperature	25ºC
Constant Filling Rate	0.000225 m³/s
Metal	Al 319
Mold Material	Furan Bonded Silica Sand
Turbulence Model	Two-equation $k-\varepsilon$ model[22]

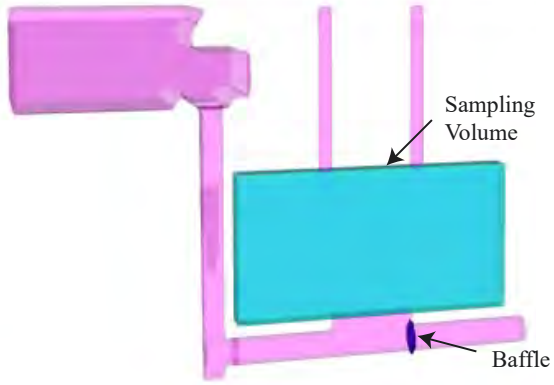

Figure 4: Image illustrating the sampling volume and baffle locations in Flow-3D Cast

4. RESULTS

The runner extension designs were evaluated based on their performance in three categories: amount of entrained air, amount of tracer, and number of void particles in the casting. Data was collected and visualized using Flow3D FlowSight, Figure 4 illustrates the casting sampling volume used for data collection.

4.1 Entrained Air

Recorded entrained air represent porosity defects caused by turbulent filling and calculated as entrained air volume

fraction, as shown in Figure 5 isosurface images. The entrained air volume fraction values at the end of the filling were used to compare the effectiveness of the runner extension designs ability to reduce porosity defects caused by turbulence. Based on the simulation data, the duckbill trap casting had the lowest entrained air volume fraction, with the fan trap casting having the highest entrained air.

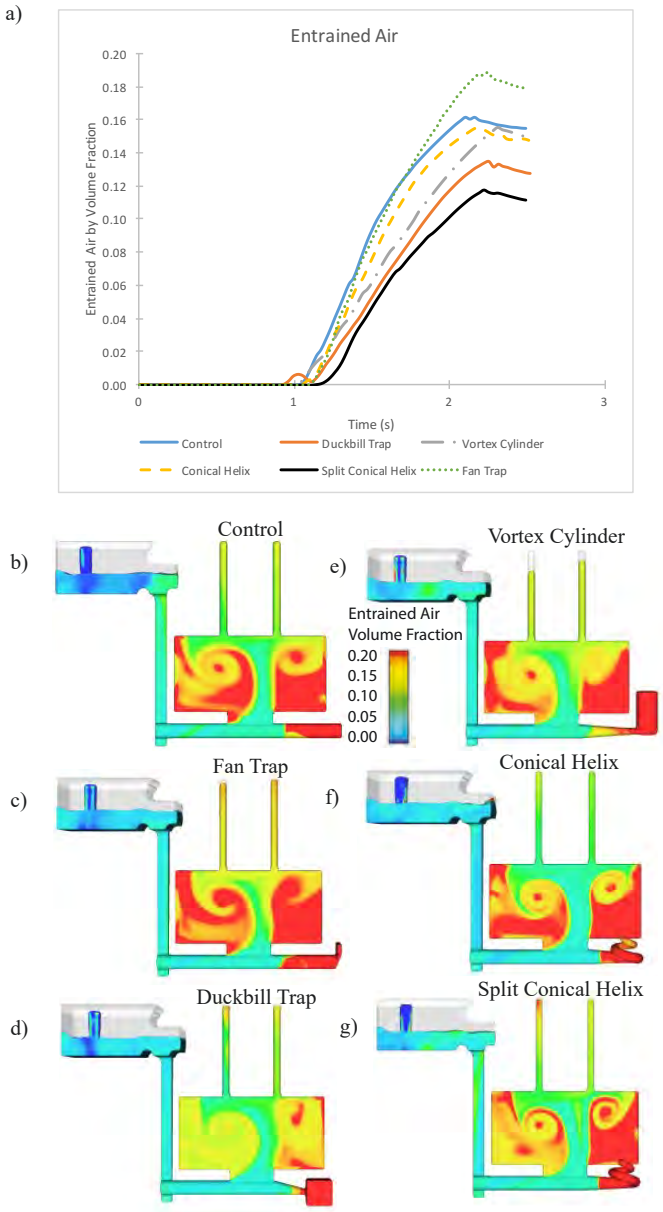

Figure 5: Graph showing entrained air volume fraction versus filling time (a), with corresponding entrained air volume fraction isosurface images at the time of completed filling: control (b), fan trap (c), duckbill trap (d), vortex cylinder (e), conical helix (f), split conical helix (g)

4.2 Tracer Content

Analysis of the tracer content in the casting evaluates the effectiveness of the runner extensions in trapping initial melt. Tracer refers to metal that has passed through the 100% porous baffle, shown in Figure 4 at the beginning of the extension, and marked as a tracer and tracked throughout the casting. In Figure 6, the tracer can be better visualized with the isosurface images. Metal that passes through the baffle is colored in and represents metal that has back flowed out of the extension into the casting. Based on the data collected, the vortex cylinder extension allowed the least amount of backflow.

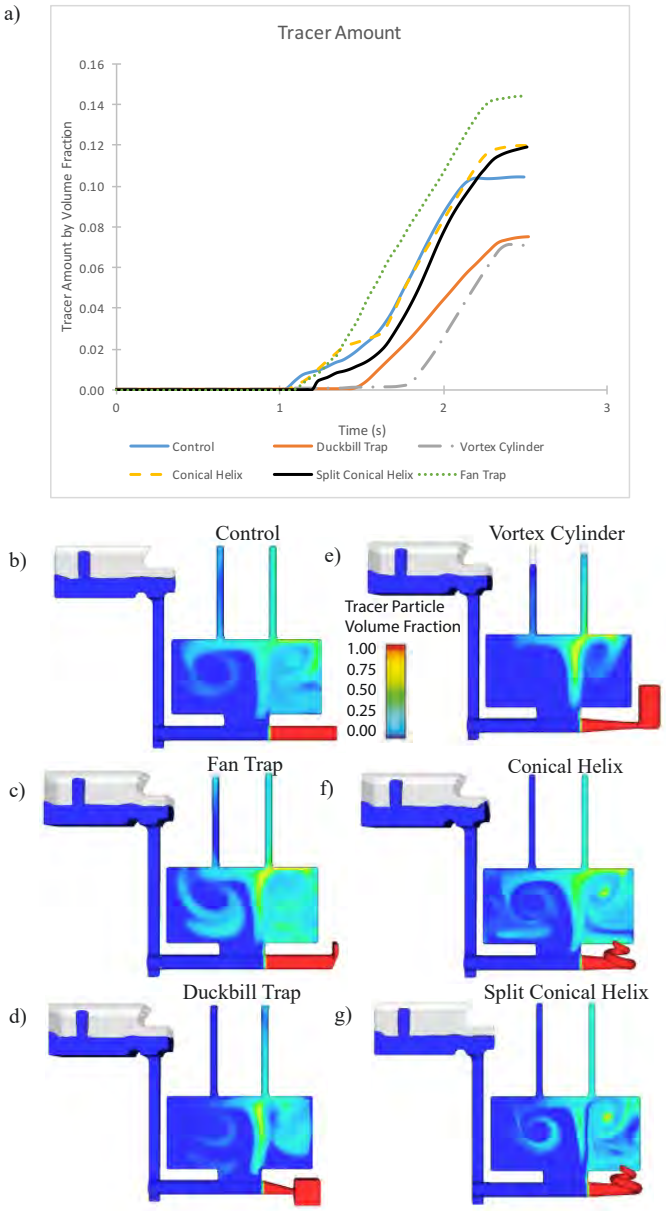

Figure 6: Graph showing the tracer amount by volume fraction versus filling time (a), with corresponding tracer volume fraction isosurface images at the time of completed filling: control (b), fan trap (c), duckbill trap (d), vortex cylinder (e), conical helix (f), split conical helix (g)

4.3 Void Particles

Figure 7 shows the location of void particles within the casting at the end of filling and does not represent the cumulative

number of voids in the casting, rather the number of voids present in the sampling volume at a given time during filling. Void particles can enter and exit the sampling volume, as well as dissipate once they reach a free surface as evident in the rapid change in voids in Figure 7(a). Only voids that are present in the casting at the end of filling are considered in this study. The simulation data indicates that the duckbill trap casting had the lowest number of void particles at the end of filling.

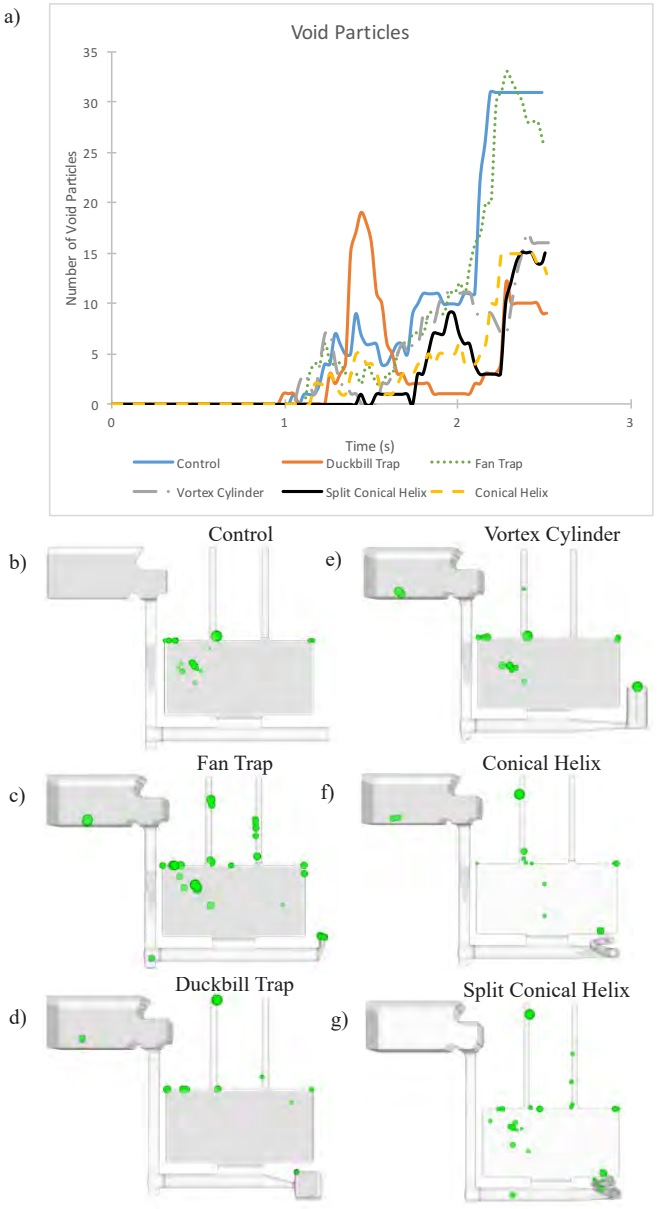

Figure 7: Graph showing number of void particles versus filling time (a), with corresponding images of void particle location at the time of completed filling: control (b), fan trap (c), duckbill trap (d), vortex cylinder (e), conical helix (f), split conical helix (g)

5. DISCUSSION

An unweighted ranking scheme was used to evaluate the overall performance of these novel runner extensions. Each design was assigned a rank based on their performance in the categories of entrained air fraction, tracer amount, number of void particles, and extension volume. A rank of 1 corresponded to the best result, with 6 representing the worst. The best extension design was the one with the smallest amount of entrained air volume fraction, tracer amount, void particles, and extension volume. The scores from each category were added to provide a total score, as shown in Table 3. Based on this analysis, the duckbill trap performed the best.

A weakness of the unweighted rank is that it doesn't take into account the quantitative differences between extension design performance. On the other hand, percent differences from the control, presented in Table 4, evaluates each extension against the control extension design within a given category.

Table 3. Unweighted ranking of the extension designs in the categories entrained air amount, tracer amount, number of void particles, and extension volume

Extension	Entrained Air	Tracer Amount	Void Particles	Extension Volume	Total Score
Control	5	3	6	2	16
Fan Trap	6	6	5	3	20
Duckbill	1	2	1	5	9
Vortex Cylinder	3	1	4	6	14
Conical Helix	2	5	2	1	10
Split Conical Helix	4	4	3	4	15

Both methods of design comparison generated similar results. Without considering extension volume, the duckbill trap extension had the best overall unweighted rank, followed by the vortex cylinder, conical helix, and split conical helix, while the fan trap was the only extension to perform worse than the control. However, when extension volume is considered, the conical helix and vortex cylinder switched rankings. When comparing extension performance to the control, the conical helix performed the best followed by the duckbill trap. This is because the conical helix was the only extension to have a lower volume (7%) compared to the control. Table 4 shows that all other extensions, besides the duckbill trap and conical helix, performed worse overall compared to the control design. However, this is misleading because when extension volume isn't considered the vortex cylinder and split conical helix are shown to perform better than the control. Extension volume is important because it has an effect on casting yield (weight of casting vs total weight poured), which is an important metric when evaluating a design's economic viability in the casting industry.

From this study, the ability of novel runner extension designs to reduce the melt velocity at the ingate and air entrainment within the casting is established. Abrupt changes in the melt velocity cause surface turbulence as well as reflecting waves. This can be better visualized in Figures 8 (a) and (b). A reflecting wave is formed due to the sudden stop in melt momentum, caused by a collision with the end of the runner

extension. This also causes a jet to occur at the ingate and could be mitigated by the use of surge control systems[9]. Both the duckbill trap and the vortex cylinder are examples of a surge control system which takes advantage of the by-pass principal described by Campbell[9]. Diverting some of the initial metal away from the ingate can assist in controlling the initial melt flow[9]. In fact the duckbill trap, vortex cylinder, conical helix, and split conical helix all utilize the by-pass principal by allowing back pressure and gate filling to occur prior to the complete filling of the extension, preventing the formation of a reflecting wave. The buildup of back pressure prior to extension filling can be seen in Figure 8 (c), (d), (e), and (f). This allows for fast priming of the runner, which impacts filling at the ingate. A computational study performed by Papanikolaou et al. on various gating designs, utilizing Flow-3D, came to similar conclusions on the importance of priming the runner for overall gating performance. They concluded that faster priming of the runner correlated to lower entrained air within the casting. However, in their study faster priming was accomplished through the use of filters[21].

Table 4. Extension design's percent difference from the control design for the categories entrained air amount, tracer amount, number of void particles, and extension volume

Extension	Entrained Air	Tracer Amount	Void Particles	Extension Volume	Total Score
Control	0%	0%	0%	0%	0%
Fan Trap	17%	33%	-16%	18%	51%
Duckbill	-16%	-31%	-71%	86%	-32%
Vortex Cylinder	-3%	-34%	-48%	104%	18%
Conical Helix	-4%	11%	-58%	-7%	-58%
Split Conical Helix	-1%	10%	-52%	61%	18%

In all of the casting simulations, some amount of tracer was present in the casting volume. This implies that impurities in the extensions may escape into the castings. However, both the duckbill trap and vortex cylinder performed better than the other designs in preventing the backflow of metal into the casting. This aligns with Komatsu's conclusion that traps with choked extensions performed better than nonchoked extensions in terms of preventing backflow[20]. This can be attributed to the narrower entrance of a choked extension connected to a trap, which helps restrict back flow, preventing reflecting waves[9]. Komatsu's report additionally concluded that larger volume traps perform better at trapping and retaining defects, which could be attributed for the vortex cylinder casting having lower tracer volume than the duckbill trap casting. Larger volumes help reduce reverse flow and provide greater space to trap inclusions [20].

The duckbill trap, vortex cylinder, conical helix, and split conical helix castings had a lower void particle count than the fan trap and control castings, shown in Table 4. The formation of void particles could be the result of air entrainment. The major factors in the observed phenomena are the by-pass principal, reflecting waves, and initial ingate flow profile as shown in Figure 8.

Even though the conical helix and split conical helix weren't the best overall designs with respect to decreasing entrained air, tracer amount, and void particles, they showed promising results. Unlike the duckbill trap and vortex cylinder, both designs didn't have a trap or flow off device. However, with higher yield volume, they were able to achieve similar results to that of the duckbill trap and vortex cylinder. They leveraged angular momentum and gravity to prevent reflecting waves and ingate jets based on the by-pass principal. The conical helix design has shown similar promise with sprue design. It was observed by Sama et al. when studying sprue designs that the conical helix sprue successfully reduced melt velocity, by converting linear velocity to angular velocity[8]. The promising results showed by the conical helix and split conical helix demonstrate that with 3DSP, novel extension designs can reduce casting defects.

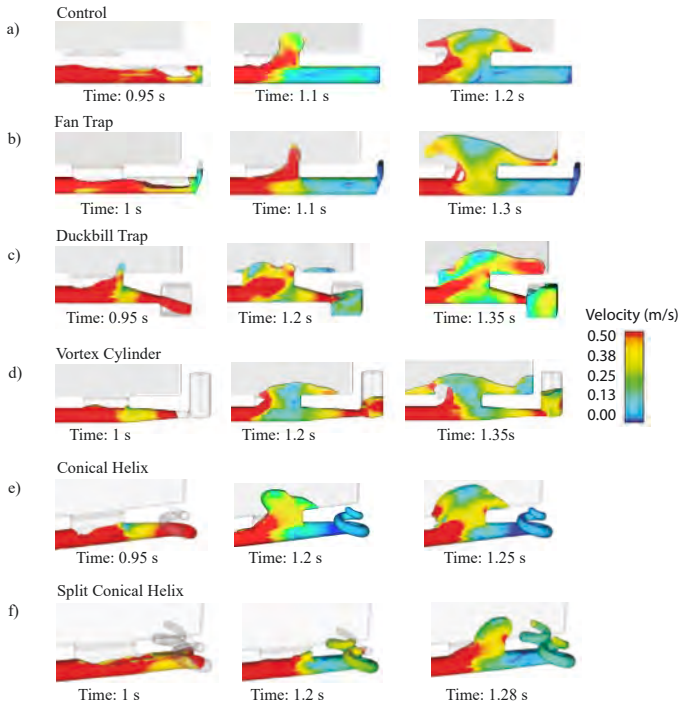

Figure 8: Velocity isosurface images from Flow Sight showing the initial ingate flow profile for the control extension (a), fan trap extension (b), duckbill trap extension (c), vortex cylinder extension (d), conical helix extension (e), split conical helix extension (f)

6. CONCLUSION

The goal of this computational study was to explore runner extension designs to better control melt filling in castings. This paper simulated a variety of both novel and existing benchmark extension designs to gain a better understanding of how they affect filling and casting quality. Novel runner extension designs were evaluated based on their ability to reduce entrained air, backflow, and void particles (bubbles) in the casting of Al 319

alloy. Based on the computational results, the main conclusions are:

(1) The duckbill trap extension was recognized as the overall best extension design based on entrained air and void particles, with a reduction of 16% entrained air and 71% void particles compared to the control design.
(2) The vortex cylinder was found to be slightly more effective (3%) at reducing tracer count compared to the duckbill trap.
(3) When comparing the novel extension designs to the control design, the conical helix had the best overall performance. This is due to a reduction in extension volume by 7% compared to the control. However, the duckbill trap performed better in all other categories.
(4) The fan trap extension performed the worst, with an increase of 17% entrained air and 33% tracer content compared to the control design .
(5) The by-pass principal and surge control systems are effective at reducing reflective waves and controlling the ingate flow profile. The duckbill trap, vortex cylinder, conical helix, and split conical helix utilized the by-pass principal. The duckbill trap and vortex cylinder are the only design groups with traps and surge control systems.
(6) Reflecting waves cause melt jetting at the ingate, which can reduce the overall casting quality.
(7) Traps and choked extensions are effective at preventing backflow and reflecting waves.
(8) The conical helix and split conical helix utilize the by-pass principal and are able control the ingate flow profile without the use of a trap or flow off device.
(9) 3D Sand Printing can be used to design complex extensions that reduce casting defects.

Future work will focus on experimentally verifying the simulation results. Additionally, optimization of the runner extension designs will be performed, to further enhance their effectiveness in reducing casting defects. Optimization will include design parameters like extension length, taper and volume, while also considering casting parameters such as flow rate, initial melt velocity, pour time, and casting yield. Since the current study did not perform design optimization, it's expected that the overall performance of the extension designs will further improve after optimization.

ACKNOWLEDGEMENTS

This work was sponsored by NSF CMMI award **#1944120.**

REFERENCES

[1] K. J. Hodder and R. J. Chalaturnyk, "Bridging additive manufacturing and sand casting: Utilizing foundry sand," *Addit. Manuf.*, vol. 28, no. June, pp. 649–660, 2019, doi: 10.1016/j.addma.2019.06.008.

[2] Evironmental Proctection Agency, "Profile of the Metal casting industry." p. 4, 1997.

[3] J. Dunham, "2019 Economic Impact of the Foundry Industry Methodology and Documentation," 2020. Accessed: Oct. 13, 2020. [Online]. Available: https://fred.stlouisfed.org/series/GDP,.

[4] M. Upadhyay, T. Sivarupan, and M. El Mansori, "3D printing for rapid sand casting—A review," *J. Manuf. Process.*, vol. 29, pp. 211–220, 2017, doi: https://doi.org/10.1016/j.jmapro.2017.07.017.

[5] E. S. Almaghariz *et al.*, "Quantifying the role of part design complexity in using 3d sand printing for molds and cores," *Int. J. Met.*, vol. 10, no. 3, pp. 240–252, 2016, doi: 10.1007/s40962-016-0027-5.

[6] L. Paul, H. C.R., W. Joseph, K. Michael, and M. Guha, "Challenges and opportunities to integrate the oldest and newest manufacturing processes: metal casting and additive manufacturing," *Rapid Prototyp. J.*, vol. 26, no. 6, pp. 1145–1154, Jan. 2020, doi: 10.1108/RPJ-10-2019-0277.

[7] S. R. Sama, J. Wang, and G. Manogharan, "Non-conventional mold design for metal casting using 3D sand-printing," *J. Manuf. Process.*, vol. 34, no. January, pp. 765–775, 2018, doi: 10.1016/j.jmapro.2018.03.049.

[8] S. R. Sama, T. Badamo, P. Lynch, and G. Manogharan, "Novel sprue designs in metal casting via 3D sand-printing," *Addit. Manuf.*, vol. 25, no. December 2018, pp. 563–578, 2019, doi: 10.1016/j.addma.2018.12.009.

[9] J. Campbell, *Castings Practice: The 10 Rules of Castings*. Elsevier, 2004.

[10] J. Campbell, "Entrainment," in *Complete Casting Handbook*, Elsevier, 2015, pp. 549–552.

[11] J. Campbell, "Filling system design fundamentals," in *Complete Casting Handbook*, Elsevier, 2011, pp. 741–756.

[12] J. Campbell, "Filling System Components," in *Complete Casting Handbook*, Elsevier, 2015.

[13] J. Campbell, "Filling system design practice," in *Complete Casting Handbook*, Elsevier, 2011, pp. 853–875.

[14] C. Reilly, N. R. Green, and M. R. Jolly, "Surface oxide film entrainment mechanisms in shape casting running systems," *Metall. Mater. Trans. B Process Metall. Mater. Process. Sci.*, vol. 40, no. 6, pp. 850–858, 2009, doi: 10.1007/s11663-009-9262-y.

[15] D. Dispinar and J. Campbell, "Porosity, hydrogen and bifilm content in Al alloy castings," *Mater. Sci. Eng. A*, vol. 528, no. 10–11, pp. 3860–3865, 2011, doi: 10.1016/j.msea.2011.01.084.

[16] J. Mi, R. A. Harding, and J. Campbell, "Effects of the entrained surface film on the reliability of castings," *Metall. Mater. Trans. A Phys. Metall. Mater. Sci.*, vol. 35 A, no. 9, pp. 2893–2902, 2004, doi: 10.1007/s11661-004-0237-y.

[17] H. Mayer, M. Papakyriacou, B. Zettl, and S. E. Stanzl-Tschegg, "Influence of porosity on the fatigue limit of die cast magnesium and aluminium alloys," *Int. J. Fatigue*, vol. 25, no. 3, pp. 245–256, 2003, doi:

10.1016/S0142-1123(02)00054-3.
[18] Y. X. Gao, J. Z. Yi, P. D. Lee, and T. C. Lindley, “A micro-cell model of the effect of microstructure and defects on fatigue resistance in cast aluminum alloys,” *Acta Mater.*, vol. 52, no. 19, pp. 5435–5449, Nov. 2004, doi: 10.1016/j.actamat.2004.07.035.
[19] X. Dai, X. Yang, J. Campbell, and J. Wood, “Effects of runner system design on the mechanical strength of Al-7Si-Mg alloy castings,” *Mater. Sci. Eng. A*, vol. 354, no. 1–2, pp. 315–325, 2003, doi: 10.1016/S0921-5093(03)00021-2.
[20] K. Ogawa, S. Kanou, and S. Kashihara, “Technical Paper Fewer Sand Inclusion Defects by CAE,” 2006.
[21] M. Papanikolaou, E. Pagone, and M. Jolly, “Running and Gating Systems,” pp. 4–15, 2020.
[22] “FLOW-3D User Manual Version 9.3,” 2008.